BBA - Molecular Basis of Disease 1865 (2019) 1253–1264

Contents lists available at ScienceDirect

BBA - Molecular Basis of Disease

journal homepage: www.elsevier.com/locate/bbadis

Nrf2 deficiency aggravates Angiotensin II-induced cardiac injury by increasing hypertrophy and enhancing IL-6/STAT3-dependent inflammation

Dandan Chen[a,1], Zhe Li[b,c,d,1], Peiqing Bao[a], Miao Chen[a], Miao Zhang[a], Fangrong Yan[e], Yitao Xu[f], Caoyu Ji[e], Xinyue Hu[a], Daniel Sanchis[g,*], Yubin Zhang[a,*], Junmei Ye[a,*]

[a] State Key Laboratory of Natural Medicines, Department of Biochemistry, School of Life Science and Technology, China Pharmaceutical University, Nanjing 210006, China
[b] Department of Cardiology, Renmin Hospital of Wuhan University, Wuhan 430060, China
[c] Cardiovascular research Institute, Wuhan University, Wuhan 430060, China
[d] Hubei key Laboratory of Cardiology, Wuhan 430060, China
[e] Research Center of Biostatistics and Computational Pharmacy, China Pharmaceutical University, Nanjing 210006, China
[f] Division of Cancer, Department of Surgery and Cancer, Imperial College London, London W120NN, United Kingdom
[g] Institut de Recerca Biomedica de Lleida (IRBLLEIDA), Universitat de Lleida, Edifici Biomedicina-I. Av. Rovira Roure, 80, 25198 Lleida, Spain

ARTICLE INFO

Keywords:
Nrf2
Heart
Hypertrophy
Inflammation
IL-6
STAT3

ABSTRACT

Background: NF-E2-related factor 2 (Nrf2) is a transcription factor playing cytoprotective effects in various pathological processes including oxidative stress and cardiac hypertrophy. Despite being a potential therapeutic target to treat several cardiomyopathies, the signaling underlying Nrf2-dependent cardioprotective action remains largely uncharacterized.

Aim: This study aimed to explore the signaling mediating the role of Nrf2 in the development of hypertensive cardiac pathogenesis by analyzing the response to Angiotensin II (Ang II) in the presence or absence of *Nrf2* expression, both in vivo and in vitro.

Results: Our results indicated that *Nrf2* deficiency exacerbated cardiac damage triggered by Ang II infusion. Mechanistically, our study shows that Ang II-triggered hypertrophy and inflammation is exacerbated in the absence of *Nrf2* expression and points to the involvement of the IL-6/STAT3 signaling pathway in this event. Indeed, our results show that IL-6 abundance triggered by Ang II is increased in the absence of *Nrf2* and demonstrate the requirement of IL-6 in STAT3 activation and cardiac inflammation induced by Ang II.

Conclusion: Our results show that Nrf2 is important for the protection of the heart against Ang II-induced cardiac hypertrophy and inflammation by mechanisms involving the regulation of IL-6/STAT3-dependent signaling.

1. Introduction

Heart failure (HF) is a debilitating disease with high rates of mortality. The pathogenesis underlying HF is complex but is mostly related to cardiac remodeling caused by cardiac myocyte hypertrophy and re-expression of the fetal gene program leading to myocardial fibrosis [1–3]. Cardiac hypertrophy is a physiological compensatory process of the heart to adapt to various pathological conditions demanding increased cardiac output. However, during maladaptive myocardial hypertrophy increased size of cardiac myocytes is accompanied of mechanic and metabolic alterations resulting in cardiac muscle dysfunction. Maladaptive hypertrophy is a frequent consequence of sustained vascular hypertension, involving Angiotensin II (Ang II) [4].

Ang II is a key executor of the renin-angiotensin-aldosterone system (RAAS), which is reported to be highly associated with increased risk of myocardial hypertrophy and HF [2,5–7] Indeed, chronic pressure overload could cause cardiac hypertrophy, which is related to the autocrine release of Ang II from the myocardium in response to abnormal harmful stress [8,9]. Accumulating evidences including ours proved that extra activated oxidative stress participates in Ang II-induced

Abbreviations: Ang II, Angiotensin II; ACE, angiotensin-converting enzyme; CK-MB, creatine kinase-MB; HF, heart failure; HO-1, heme oxygenase-1; HSD, high salt diet; LDH, lactate dehydrogenase; IL-6, Interleukin-6; RAAS, renin-angiotensin-aldosterone system; STAT3, signal transducer and activator of transcription 3; SOD1, superoxide dismutase 1; Nrf2, NF-E2-related factor 2; NRCMs, neonatal rat cardiomyocytes

* Corresponding authors.
E-mail addresses: daniel.sanchis@cmb.udl.cat (D. Sanchis), ybzhang@cpu.edu.cn (Y. Zhang), junmeiye@cpu.edu.cn (J. Ye).
[1] These authors contribute equally to this work.

https://doi.org/10.1016/j.bbadis.2019.01.020
Received 8 October 2018; Received in revised form 7 January 2019; Accepted 16 January 2019
Available online 19 January 2019
0925-4439/

cardiac myopathy [10–13]. However, it is still not fully understood how Ang II influences cardiac hypertrophy and remodeling. Investigating the downstream signals of Ang II is of potential importance because it can provide new approaches for clinical therapy of cardiovascular diseases.

The transcription factor NF-E2-related factor 2 (Nrf2) belongs to the Cap'n'collar subfamily of basic region leucine zipper transcription factors which is known to mediate protection against drug and oxidative-induced cell stress [14]. The Nrf2 pathway is involved in the cellular response to multiple diseases such as cancer [15,16], diabetes [17,18] and cardiovascular disease [19–21]. Nrf2 translocates to the nucleus upon oxidative stress, where it binds to the promoter of, among others, antioxidant genes, such as superoxide dismutase 1 (SOD1), glutathione transferases, glutamate cysteine ligase and heme oxygenase-1 (HO-1) [22]. Overexpression of *Nrf2* has been proved to be cytoprotective in multiple human diseases, whereas *Nrf2* gene deletion exacerbates the sensitivity to tissue injury [22–26]. Moreover, recent research also proved that *Nrf2* is involved in Ang II-induced as well as hemodynamic stress-induced hypertrophic cardiomyopathy [20,27,28]. Finally, *Nrf2* genetic deletion in mice has been shown to induce cardiac dysfunction and hypertrophy [29]. These results delineate a central role for *Nrf2* in preventing the heart from oxidative stress-related damage. However, the potential crosstalk between cardiac remodeling and *Nrf2* still remains poorly characterized.

Interleukin-6 (IL-6) is a pleiotropic cytokine that is produced by and acts on several tissues throughout the body including cardiomyocytes. Studies including our previous research proved that IL-6 is involved in Ang II-induced hypertensive cardiac damage [10,30–33]. The cytokines of the IL-6 family are activated in response to the phosphorylation of signal transducer and activator of transcription 3 (STAT3) [34], which promotes the transcription of inflammatory cytokines. There is co-operation of oxidative stress and inflammation induced by STAT3 activation in experimental mice hearts [35]. Our previous research also suggests alleviated oxidative stress in the heart of mice deficient for *IL-6* during Ang II-induced cardiac injury [10,30]. Moreover, it is reported that *IL-6* promoter contains an antioxidant response element (ARE) and its expression can be stimulated by *Nrf2* in β-cell of pancreas [36], implying regulatory links between these signaling pathways. However, the link between *Nrf2*-associated mitigation of oxidative stress and IL-6/STAT3-mediated stimulation of inflammation has not been tested.

In the present study, by using *Nrf2* knockout (*Nrf2* KO) mice and *IL-6* knockout (*IL-6* KO) mice, we show a previously unidentified role for *Nrf2* in agonist-induced activation of IL-6/STAT3 signaling pathway and evaluated its effect on IL-6 mediated myocardial inflammation. Our results support that *Nrf2* deficiency facilitates cardiac hypertrophy, fibrosis, oxidative stress and inflammation. We further confirmed that *Nrf2* deletion augments the elevation of IL-6 which later activates STAT3 during Ang II-induced hypertrophic cardiac injury and show the importance of IL-6 in these events.

2. Materials and methods

2.1. Animals

The investigation with experimental animals conforms to the Guide for the Care and Use of Laboratory Animals published by the US National Institutes of Health (NIH Publication No. 85-23, revised 1996) and was evaluated and approved by the Experimental Animal Ethic Committee of China Pharmaceutical University and the ethical standards in the 1964 Declaration of Helsinki and its latter amendments. *Nrf2* KO mice were a gift from Hui Xu, Medical School of Nanjing University, Nanjing, Jiangsu on a background of Balb/c. *IL-6* KO mice were purchased from Model Animal Resource Information Platform of Nanjing University (#D000054) on C57BL/6 background. All the mice used in this study were male, at the age of 3 months. The age-matched male wild-type littermates were purchased from Nanjing University (Cat No. N000013). Mice were housed in constant temperature of 22 °C in a 12/12-light/dark cycle with free access to regular rodent chow and tap water. The genotype of the animals of the colony and randomly assigned mice from the experimental groups was confirmed using PCR according to the protocols. Mice had access to regular chow (0.5% NaCl) and tap water and were allowed to adjust to the environment for at least 1 week. Then the regular chow was replaced by a high-salt diet containing 4% NaCl (Qinglongshan, Nanjing, China). Four weeks later, mice were anesthetized with 10% chloral hydrate solution (0.1 ml/20 g intraperitoneally) and osmotic minipumps (Alzet, Cupertino, California, USA) were implanted subcutaneously along the animal's dorsum under aseptic conditions to deliver either Ang II (2 mg/h per mouse, Aladdin, Shanghai, China) or vehicle (0.01-N acetic acid in saline) for 14 days. The treatment groups were as follows: WT + vehicle; *Nrf2* KO + vehicle; WT + Ang II; and *Nrf2* + AngII; WT + vehicle; *IL-6* KO + vehicle; WT + Ang II; and *IL-6* + Ang II. Treatment was continued for 5 weeks.

2.2. Echocardiography

Mice were anesthetized with isoflurane. Echocardiograms were obtained using a Vevo 2100 Ultrasound System (Visual Sonics, Toronto, Canada) equipped with a high-frequency (30 MHz) linear pediatric array transducer and was used to record a two-dimensional and M-mode echocardiogram. Hair was removed from the anterior chest using a chemical hair remover. The transducer was placed on the chest (using transducer gel as an offset), and a transthoracic echocardiogram was externally recorded. The echocardiographer was blinded to the genotype of the animal. From the M-mode echocardiogram, software on the Vevo 2100 machine was used to measure the thickness of the left ventricular (LV) posterior wall (LVPW) and the internal diameter of the LV in end-diastole (LVID-d) and end-systole (LVID-s). These values were used to automatically calculate the mass of the LV Mass, the percentage of ejection fractions and fractional shortening, and the volume of the LV in end-diastole (LV Vol-d) and end-systole (LV Vol-s) by Vevo 2100 software.

2.3. Cell culture and treatment

We obtained neonatal cardiomyocytes from the hearts of 2–4-day-old Sprague–Dawley rats after digestion with type-2 collagenase (Worthington, Lakewood, NJ, USA). We used a two-round pre-plating in order to deplete cardiomyocyte culture of non-myocardial cells. Cells were plated at a density of 10^3 cells/mm^2 in 2 g/L gelatin-coated FALCON polystyrene dishes (Becton Dickinson, Palo Alto, CA, USA) and NUNCLON four-well plates (NUNC, Roskilde, Denmark). The medium used was M199:DMEM (dulbecco's modified eagle medium) 1:3 (SIGMA-Aldrich, St. Louis, MO, USA), pH 7.2 with 7.2 mmol/L glucose, 10% horse serum and 5% fetal calf serum (Gibco, New York, NY, USA). Cardiomyocyte purity was checked by immunocytochemistry with a cardiac sarcomeric α-actinin monoclonal antibody (clone EA-53, SIGMA-Aldrich, St. Louis, MO, USA), and was found to be higher than 90% after 24 h in vitro. NRCMs were transduced with lentiviral vectors carrying short-hairpin RNA interference of *Nrf2* (sh*Nrf2*) or scrambled vector (scr). Then, NRCMs were treated with angiotensin II (Ang II) 1×10^{-7} mol/L for 24 h.

2.4. Protein extraction and Western blot analysis

Hearts were harvested, snap-frozen in liquid nitrogen and stored at −80 °C. Total proteins were extracted from heart. Tissue lysates were prepared in lysis buffer (125 mmol/l Tris, 2% SDS, pH 6.8). Approximately 30 mg of protein sample was separated via 10% SDS–PAGE and then transferred onto polyvinylidene difluoride membrane (Millipore, Bedford, Massachusetts, USA). Then the membranes were blocked with 2% BSA (bovine serum albumin) in TBST (50 mmol/

L Tris, 150 mmol/L NaCl, 0.5 mmol/L tris-buffered saline and Tween-20, pH 7.5). After blocking, the blots were incubated with the antibodies against Nrf2 (Cell Signaling Technology, CST 12721;1: 1000), STAT3 (Cell Signaling Technology, 1:2000), p-STAT3 (Cell Signaling Technology, 1:1000), GAPDH (Proteintech, 60004; 1:10000), overnight at 4 °C. Following, samples where incubated with appropriate HPR conjugated secondary antibodies. The protein bands were detected with enhanced chemiluminescence kit (Thermo Scientific, USA). The images were quantitatively analyzed by using the Image J program to make comparisons between different groups.

2.5. RNA extraction and reverse transcription-PCR analysis

Total RNA from hearts was isolated with TRIzol reagent (TransGen, ET111-01), and 1mg of RNA was reverse-transcribed using a reverse transcription system kit (Vazyme, R101-01/02). Then real-time PCR was performed with cDNA templates and SYBR Green qPCR Master Mix (Selleck, B21403) by using StepOnePlus Real-Time PCR (Applied Biosystems, Foster City, California, USA). Briefly, sequences were amplified using 5 μl Master Mix, 0.3 μl forward primer (10 pmol) of *Anf*, *Bnp*, *Collagen Iα*, *Collagen IIIα*, *Nrf2*, *matrix metalloprotein 9 (Mmp9)*, *Periostin* (Table 1), 3.9 μl nuclease-free H_2O and 0.5 μl cDNA in a total volume of 10 μl. PCR conditions were 40 cycles of 15 s at 95 °C, 30 s at 60 °C, preceded by an initial denaturation of 10 min at 95 °C and followed by a continuous melt curve from 60 to 95 °C. All samples were amplified in triplicate, and the results were normalized to the expression of *glyceraldehyde-3-phosphate dehydrogenase* (*Gapdh*). For animal tissues, two RNA preps from 4 to 6 animals (the exact number is specified in each figure) were performed, and we did triplicate of each sample for each qPCR. For cell culture, one RNA prep was performed. We did triplicate of each sample for each qPCR, and each treatment was repeated at least 3 times (specified in each figure).

2.6. Histological assessment

The middle part of the mice's hearts were fixed in 4% paraformaldehyde (PFA) for 16 h and then embedded in paraffin. Sections measuring 5 μm were cut from paraffin-embedded tissue blocks and double-stained with hematoxylin (to stain the nuclei, blue) and eosin (to outline the cardiomyocyte sectional area, red) as the H&E staining. Masson's staining for the presence of interstitial collagen fiber accumulation was a marker of cardiac fibrosis and was performed by using Masson's Staining Kit (Servicebio, Wuhan, China). The primary antibodies against CD68 (dilution 1:200; Abcam, ab955), used to detect macrophages [37,38], were applied overnight at 4 °C. After 30 min of washing, the sections were incubated with secondary antibody (Servicebio, GB23303) conjugated with horseradish peroxidase (HRP) at dilution 1:200 for 1 h at room temperature. In the next step sections were rinsed with PBS and incubated with 3, 3′-diaminobenzidinetetrahydrochloride (DAB, Dako, Copenhagen, Denmark) for 10 min. Nuclei were counterstained with hematoxylin. Negative control of staining was performed in the corresponding sections by omitting the primary antibody. These sections were scanned by the digital slide scanner NanoZoomer 2.0RS (Hamamatsu), and the area of interstitial fibrosis was calculated by Image-Pro Plus 6.0 (Media Cybernetics, Rockville, Maryland, USA).

Table 1
Primers for real-time PCR.

Target gene	Forward (5′ → 3′)	Reverse (5′ → 3′)
Anf	gtcaatcctacccccgaagcagct	cagcatgggctccttctcca
Bnp	cagctcttgaaggaccaagg	agggaagtggcaaggtaggt
Nrf2	ttctttcagcagcatcctctccac	acagccttcaatagtcccgtccag
Collagen Iα1	tgctgccttttctgttcctt	aaggtgctgggtagggaagt
Collagen IIIα1	gtccacgaggtgacaaaggt	catcttttccaggaggtcca
Mmp9	tgaatcagctggcttttgtg	gtggatagctcggtggtgtt
Periostin	aaccaaggacctgaaacacg	gtgtcaggacacggtcaatg
Il-6	cctctggtcttctggagtacc	actccttctgtgactccagc
Gapdh	ctgcgacttcaacagcaact	gagttgggatagggcctctc

2.7. Activity of manganese superoxide dismutase

Total heart was homogenized in 0.9% NaCl solution and centrifuged for 10 min at 8000 rpm. Aliquots of the supernatant were stored at −80 °C. Manganese superoxide dismutase (Mn-SOD) activity was measured by SOD Typing Assay kit (A001-2; Jiancheng bioengineer, Nanjing, China), which is based on the capacity of SOD to inhibit the auto-oxidation of hydroxylamine to nitrite and was expressed as U/mg protein. Copper–zinc superoxide dismutase (CuZn-SOD) activity was performed after pre-incubation with specific inhibitor of Mn-SOD, whereas Mn-SOD activity was calculated from the difference between total SOD and CuZn-SOD activity. Catalase (CAT) activity was measured by Catalase Assay Kit (A007-1; Jiancheng bioengineer, Nanjing, China), which is based on the measurement of the hydrogen peroxide substrate remaining after the action of CAT. Hydrogen peroxide is converted to water and oxygen by the CAT and then this enzymatic reaction is stopped with ammonium molybdate and gives a coordination complex (peroxomolybdic acid) that absorbs at 405 nm.

2.8. Malonaldehyde assay

Concentration of malonaldehyde was measured by thiobarbituric acid (TBA) method which is an index of lipid peroxidation and oxidative stress and based on the reaction of malonaldehyde with TBA at 98 °C. Briefly, an aliquot of samples (66 μl) was mixed with 66 μl of 8.1% SDS, 0.5-mlacetate buffer (0.2 M, pH 3.5), 0.5 ml 0.8% TBA and 0.2 ml water and heated at 96 °C for 30 min. After cooling to room temperature, the mix was centrifuged at -8000 rpm for 10 min. The red pigment in the supernatant was quantified by absorbance at 532 nm and then was used to calculate malondialdehyde (MDA) concentration of samples according to an MDA standard.

2.9. Elisa of plasma IL-6

In the morning, mice were anesthetized with 10% chloral hydrate solution (0.1 ml/20 g body weight, intraperitoneally), blood samples were obtained via eyeball blood collection. All blood samples without EDTA were centrifuged at 1000 *g* for 10 min at 4 °C, and the supernatant was all stored at −20 °C until analysis. ELISA kits (Beijing 4A Biotech Co. Ltd.; CME0006) were used to detect the levels of IL-6 in plasma. Samples were tested according to ELISA kit instructions. Six samples of each group were used for Elisa assay of IL-6.

2.10. Assessment of plasma LDH and CK-MB

Blood samples were collected and centrifuged at 2000 *g* at 4 °C for 20 min. Plasma was prepared and then frozen at −20 °C until further analysis. The activities of CK-MB (Shanghai MlBIO Biotechnology Co. Ltd), LDH (NanJing JianCheng) in the serum were detected with the commercially available assay kit according to the procedures.

2.11. Plasmid construction and lentvirus preparation

The 19-nucleotide sequence (5′-GCAGGACATGGATTTGATT-3′) for small interference of rat *Nrf2* was cloned into pSUPER vector (from Didier Trono, Geneva, Switzerland) using the *Bgl II* and *Hind III* sites. *Nrf2* nucleotide sequence was chosen for specific expression silencing using free RNAi design interfaces and has been validated. pSUPER or pLVTHM constructs were transfected into HEK293T packing cell line as previously described [39,40].

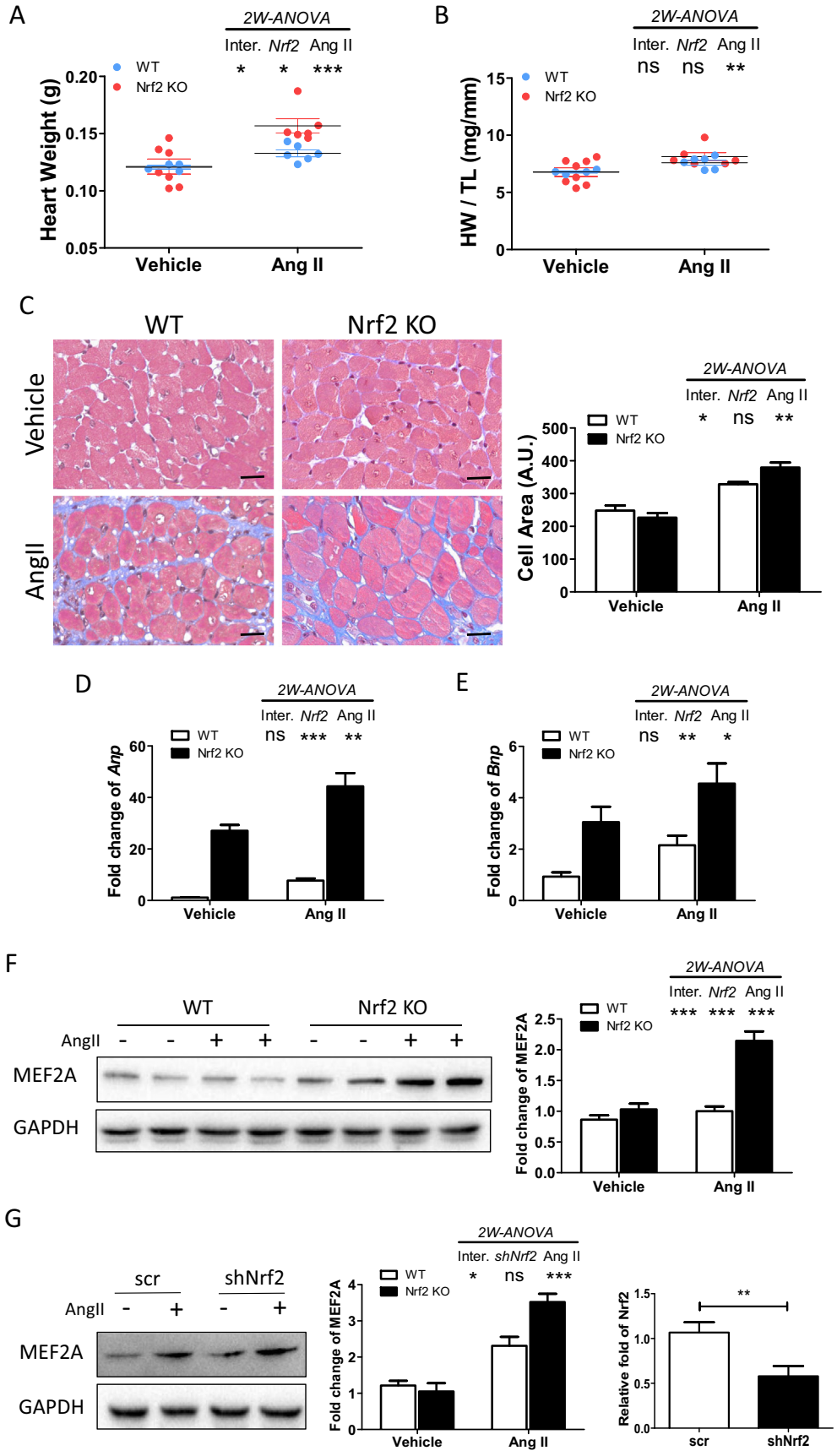

Fig. 1. The effect of *Nrf2* deficiency on Ang II-induced hypertrophic cardiomyopathy. A–B) Bar graphs showing quantitative data for HW and HW/TL; n = 6–8/group; Two-way ANOVA indicated that *Nrf2* expression and Ang II influenced HW and HW/TL. *, $p < 0.05$; **, $p < 0.01$; ***, $p < 0.001$; ns, not significant. Inter: Interaction between both variables in the experimental value; C) Representative images of Masson's trichrome staining (left panel) and calculation of transverse myocyte area of heart tissue (right panel), scale bars, 20 μm; 300 cardiomyocytes per slide, n = 4/group, 4 slides per animal; Two-way ANOVA indicated that *Nrf2* expression and Ang II influenced cell area. *, $p < 0.05$; ***, $p < 0.001$; ns, not significant; D–E) Expression of mRNA for Anp and Bnp in the heart tissue; n = 6/group; Two-way ANOVA indicated that *Nrf2* expression and Ang II influenced gene expression. *, $p < 0.05$; **, $p < 0.01$; ***, $p < 0.001$, ns, not significant; F) Western blot of MEF2A protein in the heart tissue of mice with different treatment (left panel) and protein quantification of MEF2A (right panel); n = 6/group ; Two-way ANOVA indicated that *Nrf2* expression and Ang II influenced MEF2A expression. *, $p < 0.05$; **, $p < 0.01$; ***, $p < 0.001$, ns, not significant; G) left panel: Western blot of MEF2A in NRCMs transfected with scr or sh*Nrf2* and treated with or without Ang II (100 mM) stimulation; middle panel: protein quantification of MEF2A abundance; Two-way ANOVA indicated that *Nrf2* expression and Ang II influenced MEF2A expression. *, $p < 0.05$; **, $p < 0.01$; ***, $p < 0.001$, ns, not significant. Representative western blots are shown from n = 3; right panel: real-time PCR of *Nrf2* expression in NRCMs for evaluating efficiency of *Nrf2* knockdown. Data are Mean ± SEM, *, $p < 0.05$; **, $p < 0.01$; ***, $p < 0.001$ (Student's-*t*-test).

2.12. Statistical analysis

All statistical analysis was performed using GraphPad Prism version 5.0 (GraphPad software, San Diego, CA, USA). For comparison between two groups, Student's *t*-test was performed. We performed statistical analysis with Two-way ANOVA when two conditions were involved. All statistical tests were two-sided at a significance level of 0.05.

3. Results

3.1. Nrf2 deficiency aggravates cardiac hypertrophy induced by Ang II in vivo

To assess the effect of Nrf2 on the hypertrophic response to Ang II stimulation, WT and *Nrf2* KO mice were subjected to Ang II or vehicle treatment for two weeks. *Nrf2* KO mice developed a significant increase of cardiac hypertrophy 2 weeks after Ang II stimulation compared to WT mice, as measured by the heart weight (Fig. 1A) and the ratio of heart weight/tibia length (HW/TL) (Fig. 1B), and cardiomyocyte cross-sectional area (Fig. 1C). No obvious differences were observed in the vehicle-treated WT and *Nrf2* KO mice (Fig. 1C). However, mice of both genotypes treated with Ang II showed significant increase of cardiomyocyte cross-sectional area, and cell area of cardiomyocytes from *Nrf2* KO-Ang II heart was larger than that from WT-Ang II heart, suggesting exacerbated cardiomyocyte hypertrophy induced by Ang II stimulation due to *Nrf2* deficiency.

To confirm the findings of Nrf2-mediated cardiac myocyte hypertrophy at molecular level, expression of hypertrophy-related markers, including atrial natriuretic peptide (*Anp*) and brain natriuretic peptide (*Bnp*) were assessed using tissue samples. The result showed that the expression of both genes was significantly higher in *Nrf2* KO mice than in WT mice at 2 weeks after Ang II infusion (Fig. 1D and E). We further examined expression of MEF2A, which plays pivotal role in cardiac hypertrophy [39,4041]. The results showed that MEF2A expression was significantly induced in *Nrf2* KO heart during Ang II infusion compared to other groups (Fig. 1F). In addition, the level of MEF2A protein abundance during Ang II-induced hypertrophy was higher in NRCMs transfected with lentivirus carrying short-hairpin knockdown of *Nrf2* (sh*Nrf2*) compared to those transfected with empty vector (scr) (Fig. 1G), which is in agreement with the results obtained in vivo. Together, these data imply that Nrf2 plays an important protective role against Ang II-induced cardiac hypertrophy in vivo.

3.2. Nrf2 deficiency promotes cardiac LV remodeling and dysfunction during Ang II stimulation

We next assessed cardiac function of WT and *Nrf2* KO mice and the effects of Ang II infusion by echocardiography. The increase in left ventricular (LV) mass and diastolic wall thickness (posterior wall) (LVPWd), as well as the decrease in diastolic LV chamber (interior) dimensions (LVIDd) induced by Ang II were markedly promoted in *Nrf2* KO mice compared to WT mice (Fig. 2A and Table 2). Ejection fraction (EF), an index used for assessing cardiac function, showed no statistically significant difference between WT and *Nrf2* KO mice at baseline. EF decreased in both WT and *Nrf2* KO mice after Ang II infusion for 2 weeks. However, the reduction was significantly greater in *Nrf2* KO mice compared to WT KO mice (Fig. 2A). In addition, the histological analyses based on HE staining showed larger extracellular area of damage in *Nrf2* KO mice after Ang II stimulation, as shown by discontinued cardiac myocyte connection (Fig. 2B). Moreover, serum concentrations of lactate dehydrogenase (LDH) and creatine kinase-MB (CK-MB), markers of cardiac tissue lesion, were significantly increased in *Nrf2* KO mice after 2 week's infusion of Ang II, which further confirmed the detrimental effect of *Nrf2* deficiency on cardiac function after Ang II stimulation (Fig. 2C and D).

3.3. Nrf2 deficiency augments cardiac fibrosis in response to Ang II stimulation

To further explore the mechanism by which *Nrf2* deficiency promotes cardiac hypertrophy, paraffin-embedded slides were stained with picrosirius red (PSR), and the staining was analyzed quantitatively. We observed marked interstitial and perivascular fibrosis present in the heart of *Nrf2* KO mice subjected to Ang II compared to WT-Ang II heart (Fig. 3A and B). Subsequently we analyzed gene expression levels of known mediators of fibrosis, including *collagen type I alpha 1* (*Col1a1*), *collagen type III alpha 1* (*Col3a1*), *periostin* and *matrix metalloprotein 9* (*Mmp9*). Consistent with data from quantitative analysis of fibrosis in PSR staining, the mRNA expression of these genes revealed marked elevation in *Nrf2* KO compared to WT mice after Ang II infusion (Fig. 3C, D, E and F). Together, these data indicated an anti-fibrotic effect of Nrf2, which was consistent with the histological findings of exacerbated cardiac remodeling in *Nrf2* KO mice.

3.4. Ang II stimulation in Nrf2 KO mice results in elevated cardiac oxidative stress

We next investigated *Nrf2* expression in WT mice and NRCMs treated with vehicle or Ang II. The results showed marked elevation of Nrf2 protein abundance in the heart of WT-Ang II mice and Ang II-treated NRCMs (Fig. 4A and B), suggesting the involvement of Nrf2 during Ang II-induced cardiomyopathy. To determine the role of Nrf2 in regulating Ang II-induced cardiac injury, we analyzed the expression of enzymes involved in oxidative stress, which are known targets of Nrf2. Our results revealed that the expression of manganese superoxide dismutase (MnSOD) was significantly induced in WT mice during Ang II stimulation, while abundance of MnSDO in *Nrf2* KO heart was much lower than WT heart during Ang II treatment and remained nearly at the baseline (Fig. 4C). Moreover, the abundance of malondialdehyde (MDA), a product from lipid peroxidation, increased over 2-fold during Ang II treatment in *Nrf2* KO mice (Fig. 4D). We further used the superoxide indicator DHE to detect reactive oxygen species (ROS) by immunofluorescence in NRCMs transduced with a scrambled vector (scr) or lentivirus carrying a *Nrf2*-specific short-hairpin-based silencing construct either treated with 100 nM Ang II or not. The results showed that the reduction of *Nrf2* expression augmented Ang II-induced ROS production (Fig. 4E). These data indicated that *Nrf2* deficiency inhibits anti-oxidant gene expression and promotes oxidative stress, which together contribute to cardiac maladaptative hypertrophy and dysfunction induced by Ang II.

3.5. IL-6/STAT3 signaling contributes to cardiac injury induced by Nrf2 deficiency

To assess the involvement of IL-6/STAT3 during Ang II-induced cardiac injury in mice deficient for *Nrf2*, we first examined the concentration of IL-6 in the serum of mice from the different groups. The results showed that IL-6 level was significantly higher in *Nrf2* KO mice during Ang II infusion (Fig. 5A), implying that up-regulation of IL-6 may possibly be an important mechanism of cardiac injury during Ang II stimulation in *Nrf2* KO heart. To confirm this result, we checked *Il-6* mRNA level in the heart of mice under different treatments. Our results showed that *Il-6* mRNA abundance was significantly increased in both genotypes during Ang II infusion (Fig. 5B), and *Il-6* expression in *Nrf2* KO-Ang II hearts was much higher than that in WT-Ang II heart, which is in agreement with the result of serum IL-6. To further investigate the molecular mechanisms by which *Nrf2* deficiency mediates the detrimental effect during cardiac hypertrophy, we assessed the expression of phosphorylated STAT3 (p-STAT3), which is the active form of STAT3, after Ang II infusion for 2 weeks. We observed that p-STAT3 abundance and the ratio of p-STAT3/STAT3 were significantly increased in the hearts of *Nrf2* KO mice after Ang II stimulation (Fig. 5C), indicating that

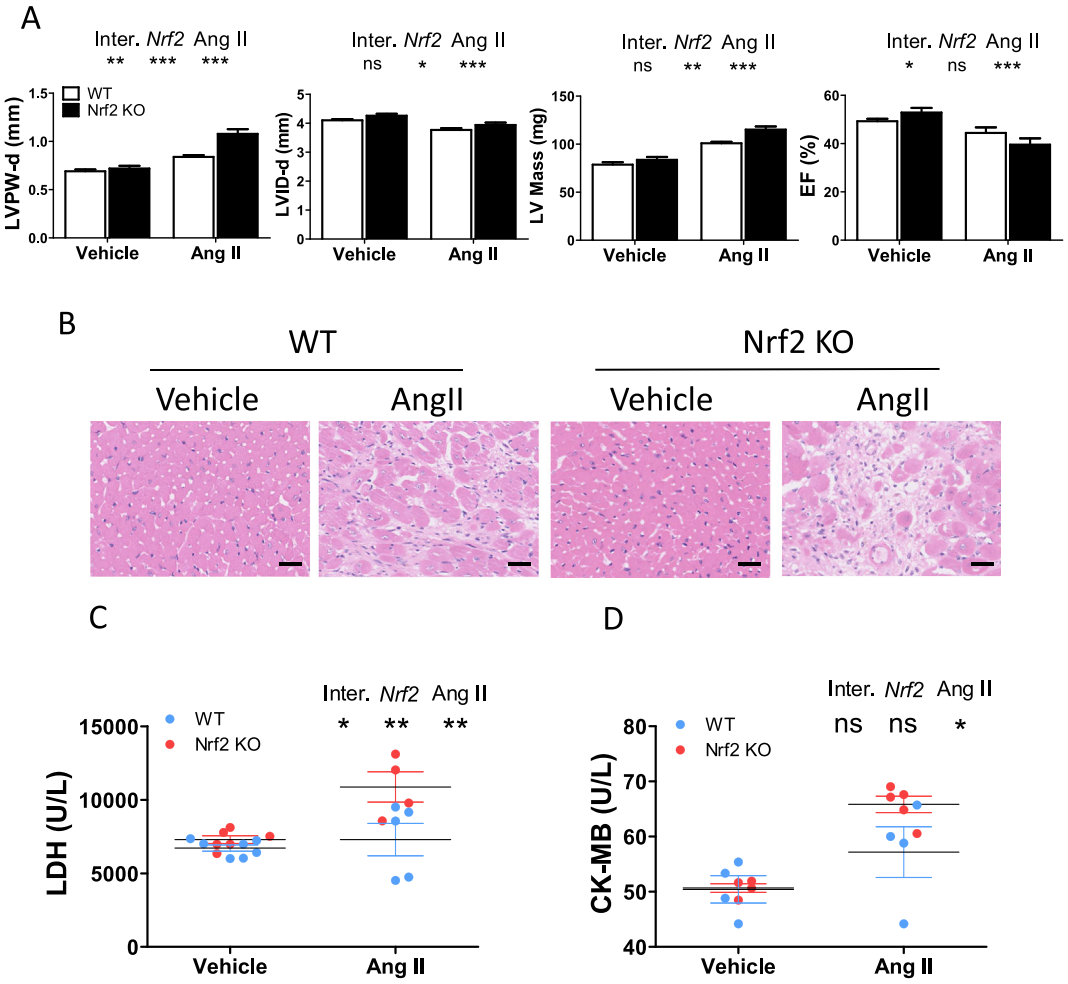

Fig. 2. The effect of *Nrf2* knockout on Ang II-induced cardiac dysfunction. A) At the end of 2-week vehicle or Ang II infusion, mice were anesthetized with isoflurane and cardiac geometry and function were evaluated using echocardiography: thickness of left ventricular posterior wall; diastolic state of left ventricular interior diameter; left ventricular mass; ejection fraction. n = 6/group; B) Representative image of H&E staining of mice heart (scale bars, 50 μm; n = 4/group); C–D) Serum concentration of LDH and CK-MB. n = 6/group. *, $p < 0.05$; **, $p < 0.01$; ***, $p < 0.001$; ns: not significant (Two-way ANOVA followed by a Bonferroni test for post-hoc analyses).

Nrf2 is involved in the tuning of Ang II-induced activation of IL-6/STAT3 signaling pathway.

To further explore the influence of Nrf2 in the inflammation process induced by Ang II, we performed immunohistochemical staining of CD68 as an indicator of macrophage infiltration, since monocytes/macrophages play a particularly important role in hypertensive cardiac injury [37,38]. The results showed that CD68-positive macrophages were more abundant in both genotypes during Ang II infusion (Fig. 5D), indicating the involvement of inflammation during Ang II-induced hypertrophic cardiac injury. Moreover, we also observed that the presence of infiltrated CD68-positive macrophages was much higher in *Nrf2* KO-Ang II heart (~3.0 fold) relative to WT-Ang II heart (~2.0 fold) (Fig. 5D), occurring in parallel to the increase of serum IL-6 level as well as p-STAT3 protein abundance in the myocardium. Thus, our data suggest that Nrf2 modulates the IL-6/STAT3 signaling pathway that is involved in the process of cardiac inflammation during Ang II-induced hypertrophy.

3.6. Ang II-induced STAT3 activation and cardiac inflammation is abrogated in mice deficient for IL-6

To determine the role of *IL-6* as well as IL-6/STAT3 signaling in Nrf2-mediated inhibition of inflammation during Ang II-induced myocardium damage, we performed immunoblotting to detect

Table 2
Echocardiographic parameters showing cardiac function in response to Ang II/HSD between genotypes.

	WT (n = 8)	WT-Ang II (n = 6)	*Nrf2* KO (n = 6)	*Nrf2* KO-Ang II (n = 6)	p value		
					Inter.	Genotype	Ang II
EF (%)	49.18 ± 1.1	42.20 ± 2.94	52.88 ± 1.90	38.78 ± 4.39	0.0337	0.7397	< 0.0001
LVID-d (mm)	4.17 ± 0.04	3.86 ± 0.10	4.26 ± 0.07	3.94 ± 0.08	0.9102	0.0188	< 0.0001
LV Mass (mg)	77.82 ± 2.9	100.7 ± 1.87	83.66 ± 3.0	116.7 ± 5.47	0.1000	0.0020	< 0.0001
LVPW-d (mm)	0.691 ± 0.02	0.866 ± 0.2	0.72 ± 0.03	1.05 ± 0.05	0.0016	0.0001	< 0.0001

Abbreviations: EF — left ventricular ejection fraction measured using Teicholz formula; LVIDd — left ventricular internal diastolic diameter; LVPWd — left ventricular posterior wall diastolic diameter (Two-way ANOVA followed by a Bonferroni test for post-hoc analyses).

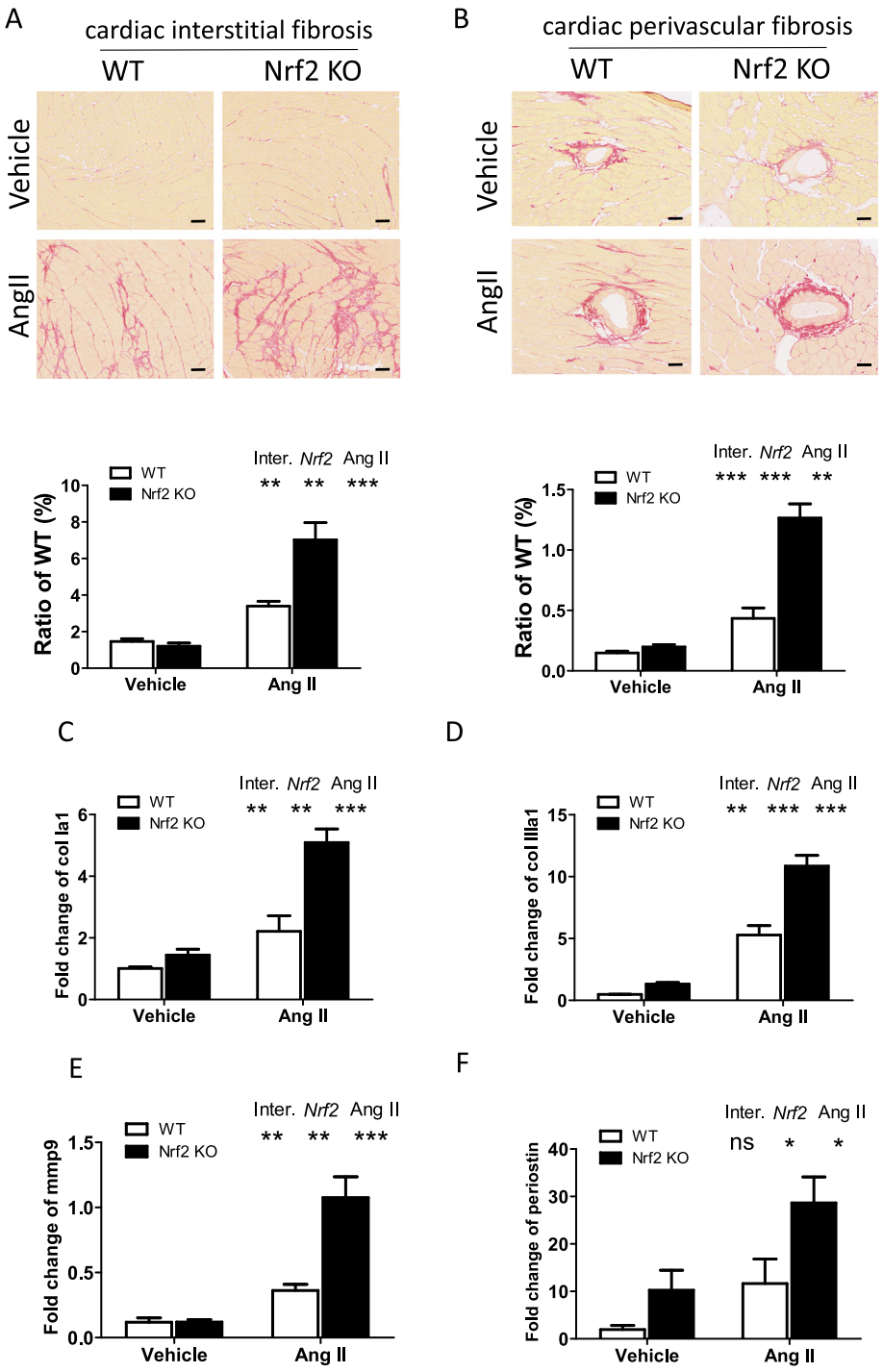

Fig. 3. The effect of *Nrf2* deficiency on cardiac hypertrophy during Ang II-stimulation. A–B) Representative images (upper panel) and quantification (lower panel) of cardiac interstitial and perivascular fibrosis (scale bars, 50 μm; n = 4/group); C–F) Expression of mRNA for *Collagen Ia1*, *Collagen Ia3*, *Mmp-9 and Periostin* in the heart tissue, n = 6/group. *, $p < 0.05$; **, $p < 0.01$; ***, $p < 0.001$; ns: not significant (Two-way ANOVA followed by a Bonferroni test for post-hoc analyses).

phosphorylation (activation) of STAT3 in the heart of wildtype and *IL-6* KO mice treated with Ang II, following the same procedure used with *Nrf2* KO mice. Our results showed that during Ang II infusion, STAT3 phosphorylation was significantly enhanced in the WT heart (Fig. 6A). On the contrary, STAT3 phosphorylation in the heart of *IL-6* knockout mice during Ang II-induced cardiac damage was very low, suggesting a key role of IL-6/STAT3 signaling pathway during Ang II-induced cardiac injury (Fig. 6A). To investigate cardiac inflammation during Ang II-infusion in the absence of *IL-6*, we assessed macrophage infiltration by CD68 staining of the heart tissue from the four groups. The results showed that, at baseline, there was no difference of CD68 staining in the heart of both genotypes (Fig. 6B). However, the presence of CD68 positive macrophages in the myocardium was significantly higher in WT-Ang II hearts compared to *IL-6* KO-Ang II hearts (Fig. 6B). The alteration of CD68 staining in the hearts of the four groups paralleled STAT3 activation status as shown in Fig. 6A. These data support the conclusion that during Ang II-induced hypertrophic cardiac injury, IL-6 plays as a key mediator in the activation of STAT3, which then promotes inflammation, which is also observed in *Nrf2* KO-Ang II hearts. On the contrary, the absence of *IL-6* could prevent Ang II-stimulated

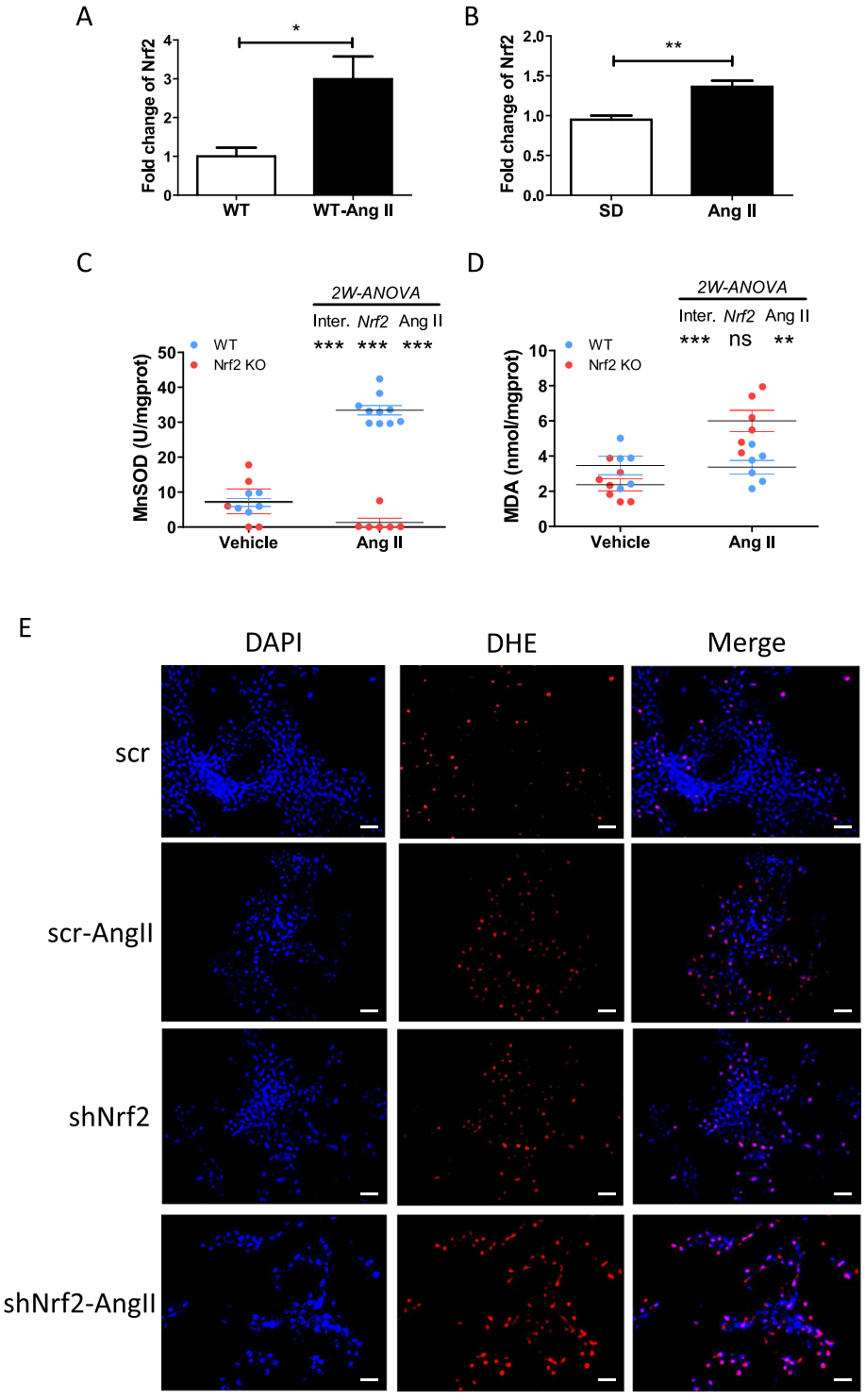

Fig. 4. Oxidative stress in the hearts of WT and *Nrf2* KO mice after two weeks of Ang II stimulation. A) real-time PCR of Nrf2 expression in the heart of WT mice with or without Ang II infusion, n = 4/group. Data are Mean ± SEM, *, $p < 0.05$ (Student's-*t*-test). B) real-time PCR of Nrf2 expression in NRCMs treated with or without 100 mM Ang II, n = 4. Data are Mean ± SEM. **, $p < 0.01$ (Student's-*t*-test); C) Concentration of Mm-SOD and D) MDA in the heart tissue of mice from four groups; n = 6/group. **, $p < 0.01$; ***, $p < 0.001$; ns: not significant (Two-way ANOVA indicated that *Nrf2* expression and Ang II influenced data); E) Immunofluorescence staining of reactive oxygen species (red) and nucleus (blue) of NRCMs transfected with scr or sh*Nrf2* lentivirus either treated with 100 nM Ang II for 24 h or not, n = 3. Scale bars, 20 μm.

STAT3 activation and myocardial inflammation.

4. Discussion

In this work we show data supporting the existence of a previously undescribed link between *Nrf2*-mediated regulation of inflammatory signaling pathway and Ang II-induced cardiac injury that involves *IL-6* and STAT3. *Nrf2* expression increased in the heart during Ang II infusion. Ang II stimulation induced more cardiac injury in mice deficient for *Nrf2* compared to wild type mice. These results provide evidence that *Nrf2* deficiency exacerbates cardiac injury during agonist-induced hypertrophic maladaptive remodeling of the heart. In addition, we also show elevated circulating *IL-6* and cardiac STAT3 activation in *Nrf2* KO-Ang II mice and demonstrate that mice lacking *IL-6* are protected against Ang II-induced inflammation. These findings highlight the potential role of *Nrf2* in attenuating agonist-induced cardiomyopathy, and its link to IL-6/STAT3 signaling during Ang II-induced cardiac injury.

During the process of cardiac adaptive remodeling to heart failure, many networks are involved, including miRNAs [42–44], metabolic molecules [45], apoptosis, inflammation, and oxidative stress. For the cardiac performance, growing, hypertrophy and remodeling until the heart failure, no data was reported about the evaluation of cardiac

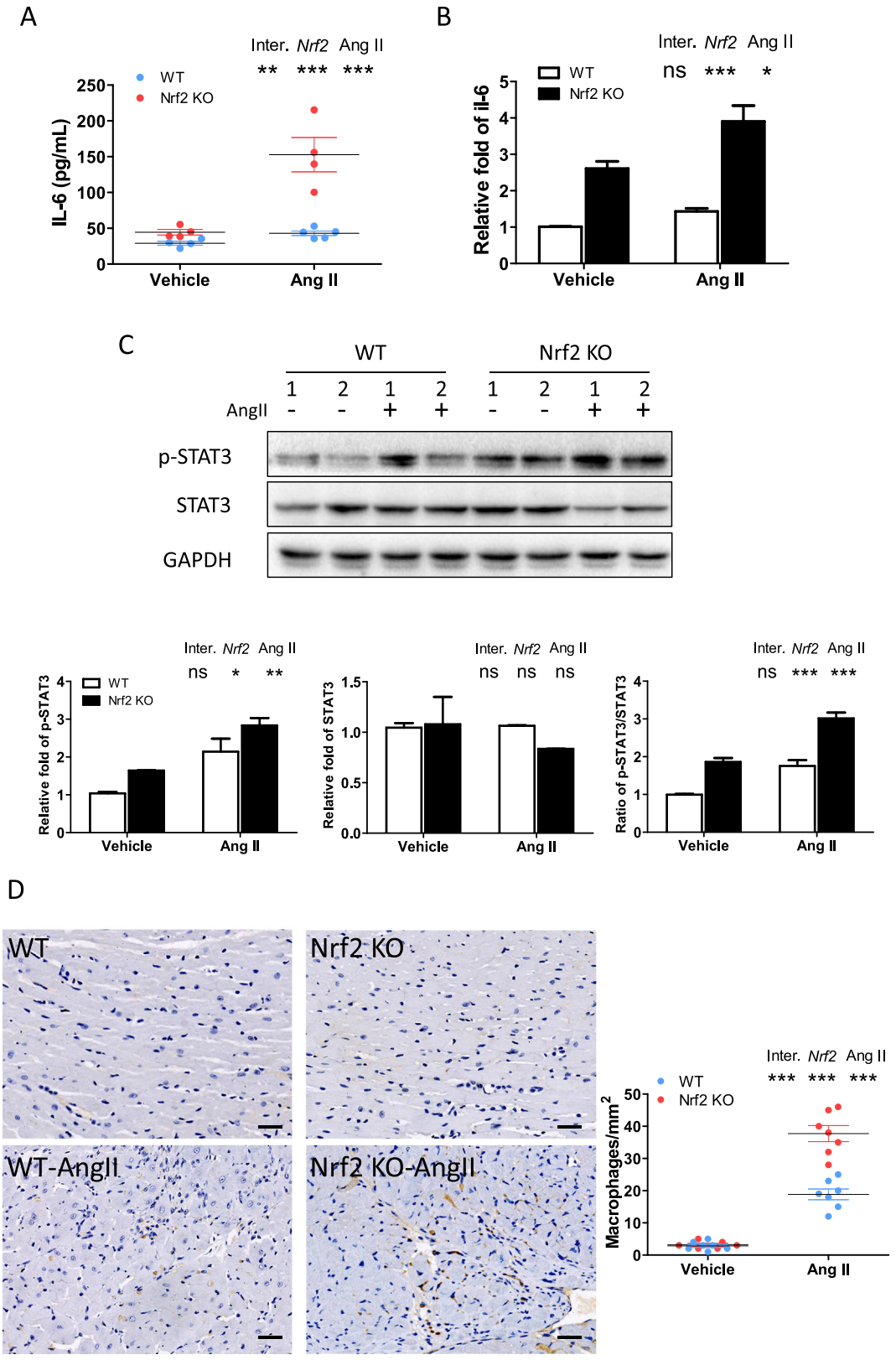

Fig. 5. Expression of IL-6 and STAT3 in the hearts of WT and *Nrf2* KO mice after Ang II infusion. A) Circulating IL-6 concentration evaluated by ELISA, n = 5; B) *Il-6* mRNA expression in mice heart with different treatment, n = 4; C) upper panel: Representative Western blots of phospho-STAT3 (p-STAT3) and STAT3 in the heart tissue. 1 and 2 represents different samples of each group. Representative western blots are shown from n = 5; lower panel: Densitometric values of protein quantification; D) left panel: Representative image of CD68 staining in the heart of mice with different treatment; right panel: CD68 quantification of the heart tissue. n = 4/group. Scale bar, 20 μm. *, $p < 0.05$; **, $p < 0.01$; ***, $p < 0.001$; ns: not significant (Two-way ANOVA followed by a Bonferroni test for post-hoc analyses).

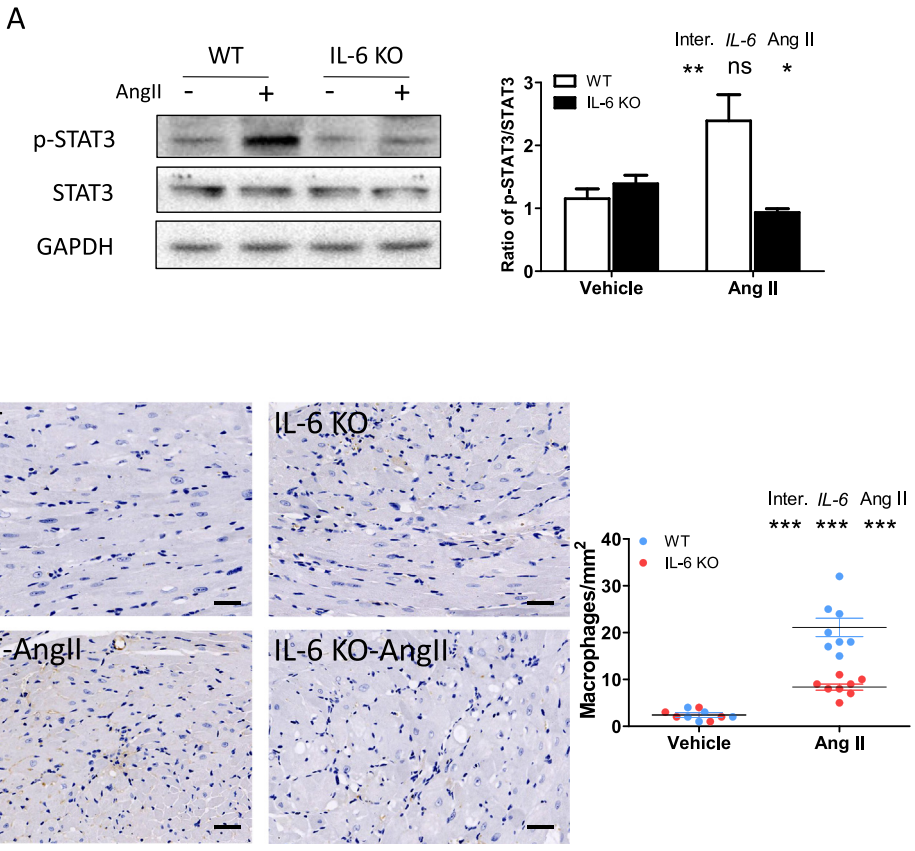

Fig. 6. Involvement of IL-6/STAT3 for Ang II-induced inflammation in cardiac myocyte. A) left panel: Representative Western blots of phospho-STAT3 (p-STAT3) and STAT3 in the heart tissue of mice with different treatments; right panel: Densitometric values of protein quantification. Representative results are shown from n = 4. B) left panel: Representative image of CD68 staining in the heart of mice with different treatment; right panel: CD68 quantification of the heart tissue. n = 4/group. Scale bar, 20 μm. *, $p < 0.05$; **, $p < 0.01$; ***, $p < 0.001$; ns: not significant (Two-way ANOVA followed by Bonferroni test for post-hoc analyses).

biomarkers as diagnostic, and monitoring markers, and prognostic markers of all the adaptive conditions [46,47,48]. *Nrf2* functions as a key player in the redox homeostatic gene regulatory network [19,20,49]. Data from *Nrf2* KO mice confirm the protective role of *Nrf2* in response to various harmful stimuli, including pressure overload-induced cardiac dysfunction, myocardial ischemia/reperfusion injury [21,27] and high glucose-induced myocardial damage via oxidative oxidation injury [50]. Moreover, oxidative stress causes the enhancement of endothelial apoptosis and contributed to a decrease in myocardial capillary density, which together result in Ang II-induced progression of cardiac injury [51]. Our results showed that there was no morphological or functional difference of the heart between WT and *Nrf2* KO mice in normal conditions. However, after Ang II infusion, *Nrf2* mRNA level was markedly induced in WT heart, suggesting its involvement during agonist-induced cardiomyopathy. In addition, our observation that increased cardiac fibrosis, hypertrophy-related biomarkers, oxidative stress, as well as serum concentration of LDH and CK-MB, which are accepted as clinical index that evaluates the degree of cardiac injury, in the heart of *Nrf2* KO mice during Ang II infusion, implied disrupted ability of compensation in response to harmful stress.

Chronic pressure overload activates left ventricular myocardial growth which then initiates and maintains a hypertrophic response [52]. In addition, blood pressure-lowering therapy reduces left ventricular mass in patients with hypertension in comparison with placebo treatment [53–55], suggesting systemic hypertension is highly correlated to cardiac hypertrophy. Taixing Cui and collages proved that *Nrf2* deficiency exacerbates Ang II-induced cardiac hypertrophy via oxidative stress-dependent down-regulation of $p27^{kip1}$ [27]. However, whether *Nrf2* deletion affects traditional hypertrophic signaling pathways remains unknown. Many signaling pathways are involved in inflammatory cardiac pathogenesis including JAK/STAT3 [56,57]. During our investigation of the molecular mechanism by which Nrf2 mediates its anti-inflammatory effects on the myocardium, we first checked circulating IL-6, a pivotal cytokine that contributes to cardiac development and the response to hypertrophic stimuli [58]. Our previous research proved that elevation of MEF2A expression is indispensable during agonist-induced hypertrophy in cardiomyocytes [40]. We observed that MEF2A protein abundance was significantly induced in the *Nrf2* KO heart compared to the WT heart after Ang II stimulation. Additionally, hypertrophic biomarkers including *Anp* and *Bnp*, were also highly induced in sh*Nrf2*-Ang II cardiomyocytes. These results indicate a correlation between cardiac hypertrophy and MEF2A expression and hypertrophy exacerbated by *Nrf2* deficiency.

To find out relevant detrimental signaling molecules involved in *Nrf2* deficiency-induced injury, *IL-6* was selected as a target because it has been implicated involving in the Nrf2 signaling pathway in other study [59]. Our results suggested that circulating IL-6 was significantly elevated in *Nrf2* KO mice during Ang II infusion, indicating the involvement of *IL-6* as well as the interaction between *Nrf2* and *IL-6* during Ang II-induced hypertrophic cardiomyopathy. Accumulating evidence suggests that the IL-6/STAT3 pathway is critical in myocardial function and cardiac protection [60–62]. We observed that there was no difference of p-STAT3 protein abundance between WT and *Nrf2* KO heart at baseline. However, after Ang II stimulation, p-STAT3 was significantly induced in *Nrf2* KO mice heart. To further investigate the activation of IL-6/STAT3 signaling pathway in *Nrf2* KO heart during Ang II-infusion, we performed CD68 staining of heart tissue from the four groups. The result suggested an elevated presence of macrophages in the *Nrf2* KO heart compared to WT during Ang II stimulation, which is consistent with the increased p-STAT3 abundance as well as p-STAT3/STAT3 ratio observed in *Nrf2* KO-Ang II hearts.

To investigate whether IL-6/STAT3 signaling is downstream of Nrf2, we also used *IL-6* KO mice treated with Ang II infusion or not, and our data showed that STAT3 activation was abrogated in the hearts deficient for *IL-6* during Ang II infusion. Additionally, the amount of CD68 positive cells was much less affected by Ang ll in the heart deficient for

IL-6 compared to the heart of WT, which supports our conclusion that Nrf2 negatively regulates IL-6/STAT3 signaling pathway during Ang II-induced hypertrophic cardiomyopathy.

In our study, by using Ang II-induced hypertensive models in vivo and in vitro, we show that Nrf2 is a negative regulator of hypertensive cardiomyopathy. The deficiency of Nrf2 promoted an inflammatory response by activating an important signaling pathway, which involves *IL-6* and STAT3 and causes cardiac inflammation. Moreover, *Nrf2* deficiency increased Ang II-induced oxidative stress. The above two effects together induce cardiac injury, therefore maladaptation and dysfunction. Our study is the first to report that genetic deletion of *Nrf2* contributes to cardiac injury via enhancing the effect of IL-6/STAT3 signaling pathway. Therefore, these findings reveal a potential role of Nrf2 in attenuating agonist-induced cardiomyopathy and its link to IL-6/STAT3 signaling during Ang II-induced cardiac injury.

Author contributions

Dandan Chen and Zhe Li performed most of the experiments; Peiqing Bao, Miao Chen, Miao Zhang, Yitao Xu, Xinyue Hu gave technical help; Fangrong Yan gave helpful suggestions and revised the artical; Daniel Sanchis gave helpful suggestions, revised the draft, and edited the language; Junmei Ye and Yubin Zhang organized the article, and Junmei Ye wrote the draft.

Funding

This work was supported by the National Natural Science Foundation of China (Grant No. 81500179, No. 81573484); Fundació La Marató de TV3 (Grant No. 20153810); the Natural Science Foundation of Jiangsu Province (Grant No. BK20150696); The Open Project of State Key Laboratory of Natural Medicines (Grant No. 3144060108); the National Found for Fostering Talents of Basic Science (NFFTBS) (Grant No. J1310032); the Priority Academic Program Development of Jiangsu Higher Education Institutions (PAPD).

Conflicts of interest

The authors declare no conflict of interest.

Transparency document

The Transparency document associated with this article can be found, in online version.

References

[1] B. Swynghedauw, Molecular Mechanisms of Myocardial Remodeling, Springer US (1999).
[2] B. Dahlof, B.R. Devereux, S.E. Kjeldsen, F.S. Group, Cardiovascular morbidity and mortality in the Losartan Intervention For End point reduction in hypertension study (LIFE): a randomised trial against atenolol, Lancet 359 (2002) 995–1003.
[3] B. Swynghedauw, C. Delcayre, J.L. Samuel, A. Mebazaa, A. Cohensolal, Molecular mechanisms in evolutionary cardiology failure, Ann. N. Y. Acad. Sci. 1188 (2010) 58.
[4] L.S.P. Diaz, M.L. Schuman, M. Aisicovich, J.E. Toblli, C.J. Pirola, M.S. Landa, S.I. Garcia, Angiotensin II requires an intact cardiac thyrotropin-releasing hormone (TRH) system to induce cardiac hypertrophy in mouse, J. Mol. Cell. Cardiol. 24 (2018) 1–11 (Nov).
[5] P.C. Group, Randomised trial of a perindopril-based blood-pressure-lowering regimen among 6,105 individuals with previous stroke or transient ischaemic attack, Lancet 358 (2001) 1033.
[6] K.M. Fox, Efficacy of perindopril in reduction of cardiovascular events among patients with stable coronary artery disease: randomised, double-blind, placebo-controlled, multicentre trial (the EUROPA study), Lancet 362 (2003) 782–788.
[7] S. Yusuf, P. Sleight, J. Pogue, J. Bosch, R. Davies, G. Dagenais, Effects of an angiotensin-converting-enzyme inhibitor, ramipril, on cardiovascular events in high-risk patients. The Heart Outcomes Prevention Evaluation Study Investigators, N. Engl. J. Med. 342 (2000) 145–153.
[8] J. Sadoshima, Y. Xu, H.S. Slayter, S. Izumo, Autocrine release of angiotensin II mediates stretch-induced hypertrophy of cardiac myocytes in vitro, Cell 75 (1993) 977.
[9] P.H. Sugden, Mechanotransduction in Cardiomyocyte Hypertrophy, Circulation 103 (2001) 1375–1377.
[10] S. Yang, D. Chen, F. Chen, X. Zhao, Y. Zhang, Z. Li, L. Jin, Y. Xu, D. Sanchis, J. Ye, Deletion of protein kinase B2 preserves cardiac function by blocking interleukin-6-mediated injury and restores blood pressure during angiotensin II/high-salt-diet-induced hypertension, J. Hypertens. 36 (4) (2018) 834–846 (Apr).
[11] G.I. Al, D.N. Meijles, S. Mutchler, Q. Zhang, S. Sahoo, A. Gorelova, A.J. Henrich, A.I. Rodríguez, T. Mamonova, G.J. Song, Binding of EBP50 to Nox organizing subunit p47phox is pivotal to cellular reactive species generation and altered vascular phenotype, Proc. Natl. Acad. Sci. U. S. A. 113 (2016) E5308.
[12] Y.S. Choi, A.B. de Mattos, D. Shao, T. Li, M. Nabben, M. Kim, W. Wang, R. Tian, K.S. Jr, Preservation of myocardial fatty acid oxidation prevents diastolic dysfunction in mice subjected to angiotensin II infusion, J. Mol. Cell. Cardiol. 100 (2016) 64–71.
[13] T. Takayanagi, T. Kawai, S.J. Forrester, T. Obama, T. Tsuji, Y. Fukuda, K.J. Elliott, D.G. Tilley, R.L. Davisson, J.Y. Park, Role of epidermal growth factor receptor and endoplasmic reticulum stress in vascular remodeling induced by angiotensin II, Hypertension 65 (2015) 1349–1355.
[14] A. Lau, T. Wang, S.A. Whitman, D.D. Zhang, The predicted molecular weight of Nrf2: it is what it is not, Antioxid. Redox Signal. 18 (2013) 91.
[15] M. Rojo de la Vega, E. Chapman, D.D. Zhang, NRF2 and the hallmarks of cancer, Cancer Cell. 34 (1) (2018) 21–43 (Jul 9).
[16] S.A. Best, D.P.D. Souza, A. Kersbergen, A.N. Policheni, S. Dayalan, D. Tull, V. Rathi, D.H. Gray, M.E. Ritchie, M.J. Mcconville, Synergy between the KEAP1/NRF2 and PI3K pathways drives non-small-cell lung cancer with an altered immune microenvironment, Cell Metab. 27 (2018) 935.
[17] D.V. Chartoumpekis, Y. Yagishita, M. Fazzari, D.L. Palliyaguru, U.N. Rao, A. Zaravinos, N.K. Khoo, F.J. Schopfer, K.R. Weiss, G.K. Michalopoulos, Nrf2 prevents Notch-induced insulin resistance and tumorigenesis in mice, JCI Insight 3 (2018).
[18] O. Kuda, M. Brezinova, J. Silhavy, V. Landa, V. Zidek, C. Dodia, F. Kreuchwig, M. Vrbacky, L. Balas, T. Durand, Nrf2-mediated antioxidant defense and peroxiredoxin 6 are linked to biosynthesis of palmitic acid ester of 9-hydroxystearic acid, Diabetes 67 (6) (2018) 1190–1199 (Jun).
[19] W. Wang, S. Li, H. Wang, B. Li, L. Shao, Y. Lai, G. Horvath, Q. Wang, M. Yamamoto, J.S. Janicki, Nrf2 enhances myocardial clearance of toxic ubiquitinated proteins, J. Mol. Cell. Cardiol. 72 (2014) 305–315.
[20] J. Li, C. Zhang, Y. Xing, J.S. Janicki, M. Yamamoto, X.L. Wang, D.Q. Tang, T. Cui, Up-regulation of p27kip1 contributes to Nrf2-mediated protection against angiotensin II-induced cardiac hypertrophy, Carbohydr. Res. 90 (2011) 315–324.
[21] Q. Qin, Q. Chen, T. Niu, H. Zang, Q. Lei, L. Lyu, X. Wang, M. Nagarkatti, P. Nagarkatti, J.S. Janicki, Nrf2-mediated cardiac maladaptive remodeling and dysfunction in a setting of autophagy insufficiency, Hypertension 67 (2015) 107.
[22] J.M. Lee, M.J. Calkins, K. Chan, Y.W. Kan, J.A. Johnson, Identification of the NF-E2-related Factor-2-dependent genes conferring protection against oxidative stress in primary cortical astrocytes using oligonucleotide microarray analysis, J. Biol. Chem. 278 (2003) 12029–12038.
[23] T. Nguyen, P. Nioi, C.B. Pickett, The Nrf2-antioxidant response element signaling pathway and its activation by oxidative stress, J. Biol. Chem. 284 (2009) 13291–13295.
[24] W. Li, A.N. Kong, Molecular mechanisms of Nrf2-mediated antioxidant response, Mol. Carcinog. 48 (2009) 91.
[25] Q. Ma, Role of Nrf2 in oxidative stress and toxicity, Annu. Rev. Pharmacol. Toxicol. 53 (2013) 401–426.
[26] T.W. Kensler, N. Wakabayashi, S. Biswal, Cell survival responses to environmental stresses via the Keap1-Nrf2-ARE pathway, Annu. Rev. Pharmacol. Toxicol. 47 (2006) 89–116.
[27] J. Li, T.L. Ichikawa, Nrf2 protects against maladaptive cardiac responses to hemodynamic stress, Arterioscler. Thromb. Vasc. Biol. 29 (2009) 1843.
[28] M. Barančík, L. Grešová, M. Barteková, I. Dovinová, Nrf2 as a key player of redox regulation in cardiovascular diseases, Physiol. Res. 65 (Suppl. 1) (2016) S1.
[29] R. Erkens, C.M. Kramer, W. Lückstädt, C. Panknin, L. Krause, M. Weidenbach, J. Dirzka, T. Krenz, E. Mergia, T. Suvorava, Left ventricular diastolic dysfunction in Nrf2 knock out mice Is associated with cardiac hypertrophy, decreased expression of SERCA2a, and preserved endothelial function, Free Radic. Biol. Med. 89 (2015) 906–917.
[30] F. Chen, D. Chen, Y. Zhang, L. Jin, H. Zhang, M. Wan, T. Pan, X. Wang, Y. Su, Y. Xu, J. Ye, Interleukin-6 deficiency attenuates angiotensin II-induced cardiac pathogenesis with increased myocyte hypertrophy, Biochem. Biophys. Res. Commun. 494 (2017) 534–541.
[31] S. Fredj, J. Bescond, C. Louault, A. Delwail, J.C. Lecron, D. Potreau, Role of interleukin-6 in cardiomyocyte/cardiac fibroblast interactions during myocyte hypertrophy and fibroblast proliferation, J. Cell. Physiol. 204 (2005) 428–436.
[32] M. Sano, K. Fukuda, H. Kodama, T. Takahashi, T. Kato, D. Hakuno, T. Sato, T. Manabe, S. Tahara, S. Ogawa, Autocrine/Paracrine secretion of IL-6 family cytokines causes angiotensin II-induced delayed STAT3 activation, Biochem. Biophys. Res. Commun. 269 (2000) 798–802.
[33] D.L. Mann, Stress-activated cytokines and the heart: from adaptation to maladaptation, Annu. Rev. Physiol. 65 (2003) 81–101.
[34] X.O. Yang, A.D. Panopoulos, R. Nurieva, S.H. Chang, D. Wang, S.S. Watowich, C. Dong, STAT3 regulates cytokine-mediated generation of inflammatory helper T cells, J. Biol. Chem. 282 (2007) 9358–9363.
[35] R. Loperena, J.P. Van Beusecum, H.A. Itani, N. Engel, F. Laroumanie, L. Xiao, F. Elijovich, C.L. Laffer, J.S. Gnecco, J. Noonan, Hypertension and increased endothelial mechanical stretch promote monocyte differentiation and activation:

Roles of STAT3, interleukin 6 and hydrogen peroxide, Cardiovasc. Res. 114 (11) (2018) 1547–1563 (Sep 1).
[36] C.J. Wruck, K. Streetz, G. Pavic, M.E. Götz, M. Tohidnezhad, L.O. Brandenburg, D. Varoga, O. Eickelberg, T. Herdegen, C. Trautwein, Nrf2 induces interleukin-6 (IL-6) expression via an antioxidant response element within the IL-6 promoter, J. Biol. Chem. 286 (2011) 4493–4499.
[37] K. Minami, K. Hiwatashi, S. Ueno, M. Sakoda, S. Iino, H. Okumura, M. Hashiguchi, Y. Kawasaki, H. Kurahara, Y. Mataki, Prognostic significance of CD68, CD163 and folate receptor-β positive macrophages in hepatocellular carcinoma, Exp. Ther. Med. 15 (2018).
[38] L. Boytard, R. Spear, G. Chinetti-Gbaguidi, A.E. Acosta-Martin, J. Vanhoutte, N. Lamblin, B. Staels, P. Amouyel, S. Haulon, F. Pinet, Role of proinflammatory CD68(+) mannose receptor(−) macrophages in peroxiredoxin-1 expression and in abdominal aortic aneurysms in humans, Arterioscler. Thromb. Vasc. Biol. 33 (2013) 431–438.
[39] D. Chen, F. Chen, Y. Xu, Y. Zhang, Z. Li, H. Zhang, T. Pan, Y. Su, M. Wan, X. Wang, J. Ye, AKT2 deficiency induces retardation of myocyte development through EndoG-MEF2A signaling in mouse heart, Biochem. Biophys. Res. Commun. 493 (4) (2017) 1410–1417 (Dec 2).
[40] J. Ye, M. Cardona, M. Llovera, J.X. Comella, D. Sanchis, Translation of myocyte enhancer factor-2 is induced by hypertrophic stimuli in cardiomyocytes through a calcineurin-dependent pathway, J. Mol. Cell. Cardiol. 53 (2012) 578–587.
[41] F.J. Naya, B.L. Black, H. Wu, R. Bassel-duby, J.A. Richardson, J.A. Hill, E.N. Olson, Mitochondrial deficiency and cardiac sudden death in mice lacking the MEF2A transcription factor, Nat. Med. 8 (2002) 1303–1309.
[42] R. Marfella, C. Filippo, N. Potenza, C. Sardu, M.R. Rizzo, M. Siniscalchi, E. Musacchio, M. Barbieri, C. Mauro, N. Mosca, F. Solimene, M.T. Mottola, A. Russo, F. Rossi, G. Paolisso, M. D'Amico, Circulating microRNA changes in heart failure patients treated with cardiac resynchronization therapy: responders vs. non-responders, Eur. J. Heart Fail. 15 (2013).
[43] C. Sardu, R. Marfella, G. Santulli, G. Paolisso, Functional role of miRNA in cardiac resynchronization therapy, Pharmacogenomics 15 (2014).
[44] C. Sardu, M. Barbieri, M.R. Rizzo, P. Paolisso, G. Paolisso, R. Marfella, Cardiac resynchronization therapy outcomes in type 2 diabetic patients: role of microRNA changes, J. Diabetes Res. 2016 (2016).
[45] C. Sardu, P. Paolisso, C. Sacra, M. Santamaria, C. de Lucia, A. Ruocco, C. Mauro, G. Paolisso, M.R. Rizzo, M. Barbieri, R. Marfella, Cardiac resynchronization therapy with a defibrillator (CRTd) in failing heart patients with type 2 diabetes mellitus and treated by glucagon-like peptide 1 receptor agonists (GLP-1 RA) therapy vs. conventional hypoglycemic drugs: arrhythmic burden, hospitalizations for heart failure, and CRTd responders rate, Cardiovasc. Diabetol. 17 (2018) 137.
[46] C. Sardu, G. Pieretti, N. D'Onofrio, F. Ciccarelli, P. Paolisso, M.B. Passavanti, R. Marfella, M. Cioffi, P. Mone, A.M. Dalise, F. Ferraraccio, I. Panarese, A. Gambardella, N. Passariello, M.R. Rizzo, M.L. Balestrieri, G. Nicoletti, M. Barbieri, Inflammatory cytokines and SIRT1 levels in subcutaneous abdominal fat: relationship with cardiac performance in overweight pre-diabetics patients, Front. Physiol. 9 (2018) 1030.
[47] M.L. Vicario, P. Caso, A.R. Martiniello, L. Fontanella, M. Petretta, C. Sardu, M.P. Petretta, D. Bonaduce, Effects of volume loading on strain rate and tissue Doppler velocity imaging in patients with idiopathic dilated cardiomyopathy, J. Cardiovasc. Med. (Hagerstown) 7 (2006) 852–858.
[48] C. Sardu, R. Marfella, M. Santamaria, S. Papini, Q. Parisi, C. Sacra, D. Colaprete, G.G. Paolisso, M.R. Rizzo, M. Barbieri, Stretch, injury and inflammation markers evaluation to predict clinical outcomes after implantable cardioverter defibrillator therapy in heart failure patients with metabolic syndrome, Front. Physiol. 9 (2018) 758.
[49] T. Ichikawa, J. Li, C.J. Meyer, J.S. Janicki, M. Hannink, T. Cui, Dihydro-CDDO-trifluoroethyl amide (dh404), a novel Nrf2 activator, suppresses oxidative stress in cardiomyocytes, PLoS One 4 (2009) e8391.
[50] X. He, H. Kan, L.Q. Ma, Nrf2 is critical in defense against high glucose-induced oxidative damage in cardiomyocytes, J. Mol. Cell. Cardiol. 46 (2009) 47–58.
[51] H. Nako, K. Kataoka, N. Koibuchi, Y.F. Dong, K. Toyama, E. Yamamoto, O. Yasuda, H. Ichijo, H. Ogawa, S. Kim-Mitsuyama, Novel mechanism of angiotensin II-induced cardiac injury in hypertensive rats: the critical role of ASK1 and VEGF, Hypertens. Res. 35 (2012) 194–200.
[52] E.Z. Soliman, R.J. Prineas, Antihypertensive therapies and left ventricular hypertrophy, Curr. Hypertens. Rep. 19 (2017) 79.
[53] R.H. Fagard, H. Celis, L. Thijs, S. Wouters, Regression of left ventricular mass by antihypertensive treatment: a meta-analysis of randomized comparative studies, Hypertension 54 (2009) 1084–1091.
[54] B. Dahlof, H. Herlitz, M. Aurell, L. Hansson, Reversal of cardiovascular structural changes when treating essential hypertension. The importance of the renin-angiotensin-aldosterone system, Am. J. Hypertens. 5 (1992) 900–911.
[55] R.E. Schmieder, P. Martus, A. Klingbeil, Reversal of left ventricular hypertrophy in essential hypertension. A meta-analysis of randomized double-blind studies, JAMA 275 (1996) 1507–1513.
[56] Z. Wang, J. Yu, J. Wu, F. Qi, H. Wang, Z. Wang, Z. Xu, Scutellarin protects cardiomyocyte ischemia–reperfusion injury by reducing apoptosis and oxidative stress, Life Sci. 157 (2016) 200–207.
[57] J.D. Drenckhahn, J. Strasen, K. Heinecke, P. Langner, K.V. Yin, F. Skole, M. Hennig, B. Spallek, R. Fischer, F. Blaschke, A. Heuser, T.C. Cox, M.J. Black, L. Thierfelder, Impaired myocardial development resulting in neonatal cardiac hypoplasia alters postnatal growth and stress response in the heart, Cardiovasc. Res. 106 (2015) 43–54.
[58] J. Xu, N.L. Gong, I. Bodi, B.J. Aronow, P.H. Backx, J.D. Molkentin, Myocyte enhancer factors 2A and 2C induce dilated cardiomyopathy in transgenic mice, J. Biol. Chem. 281 (2006) 9152.
[59] N. Kweider, A. Fragoulis, C. Rosen, U. Pecks, W. Rath, T. Pufe, C.J. Wruck, Interplay between vascular endothelial growth factor (VEGF) and nuclear factor erythroid 2-related factor-2 (Nrf2): implications for preeclampsia, J. Biol. Chem. 286 (2011) 42863–42872.
[60] U.A.K. Betz, W. Bloch, M.V.D. Broek, K. Yoshida, T. Taga, T. Kishimoto, K. Addicks, K. Rajewsky, W. Müller, Postnatally induced inactivation of gp130 in mice results in neurological, cardiac, hematopoietic, immunological, hepatic, and pulmonary defects, J. Exp. Med. 188 (1998) 1955–1965.
[61] D. Hilfiker-Kleiner, A. Hilfiker, M. Fuchs, K. Kaminski, A. Schaefer, B. Schieffer, A. Hillmer, A. Schmiedl, Z. Ding, E. Podewski, Signal transducer and activator of transcription 3 is required for myocardial capillary growth, control of interstitial matrix deposition, and heart protection from ischemic injury, Circ. Res. 95 (2004) 187–195.
[62] H. Hirota, J. Chen, U.A. Betz, K. Rajewsky, Y. Gu, J. R Jr., W. Müller, K.R. Chien, Loss of a gp130 cardiac muscle cell survival pathway is a critical event in the onset of heart failure during biomechanical stress, Cell 97 (1999) 189–198.